Inorg. Chem. **2008**, *47*, 429–438

$RhCl_3$-Assisted C–H and C–S Bond Scissions: Isomeric Self-Association of Organorhodium(III) Thiolato Complex. Synthesis, Structure, and Electrochemistry

Kausikisankar Pramanik,*,† Ujjwal Das,† Basab Adhikari,† Deepak Chopra,‡ and Helen Stoeckli-Evans§

Department of Chemistry, Inorganic Chemistry Section, Jadavpur University, Kolkata 700032, India, Solid State and Structural Chemistry Unit, Indian Institute of Science, Bangalore 560012, India, and Institut de Chemie, Université de Neuchâtel, Av. de Bellevaux 51, 2000, Neuchâtel, Switzerland

Received August 11, 2007

The ligating properties of alkyl 2-(phenylazo)phenyl thioether **1** (HL^R; R = Me, CH_2Ph) toward Rh(III) have been examined. A novel hexacoordinated orthometalated rhodium(III) thiolato complex *trans*-$[Rh(L)Cl(PPh_3)_2]$ **5** has been synthesized from **1** and $RhCl_3 \cdot 3H_2O$ in the presence of excess PPh_3 via in situ $C(sp^2)$–H and $C(sp^3)$–S bond scissions, which is the first example for a coordination compound of $[L]^{2-}$. We were also able to isolate the intermediate organothioether rhodium(III) compound *trans*-$[Rh(L^R)Cl_2(PPh_3)]$ **6** with 1 equiv of PPh_3 relative to both **1** and $RhCl_3 \cdot 3H_2O$ in the course of the synthesis of the S-dealkylated product. PPh_3 plays a crucial role in the $C(sp^3)$–S cleavage process. A plausible mechanistic pathway is presented for C–S bond cleavage, and reductive cleavage by single-electron transfer mechanism is likely to be operative. The electronically and coordinatively saturated thiolato complex **5**, indefinitely stable in the solid state, undergoes spontaneous self-dimerization in solution via dissociation of one coordinated PPh_3 molecule to afford edge-shared bioctahedral *anti*-$[Rh(L)Cl(PPh_3)]_2$ **7** and *syn*-$[Rh(L)Cl(PPh_3)]_2$ **8** isomers. All the synthesized organosulfur rhodium(III) compounds were isolated as both air- and moisture-stable solids and spectroscopically characterized in both solution and solid states. In addition, all the representative members have been authenticated by single-crystal X-ray structure analyses. Availability of the isomeric dimers provides an opportunity to recognize the presence of noncovalent intramolecular "*metallochelate–metallochelate*" interaction in the sterically encumbered syn isomer. Unlike other organosulfur rhodium complexes, the monomeric thiolato complex **5** exhibits a fully reversible oxidative wave at 0.82 V vs Ag/AgCl, which is supposed to be primarily centered on the thiolato sulfur atom, and such perception is consistent with the DFT study. Formation of rhodium-bound thiyl radical cation $\mathbf{5}^{\bullet+}$ by electrochemical oxidation was scrutinized by EPR spectroscopy.

Introduction

Platinum group metals display efficacy in various organic transformations via activation of C−H and C−S bonds; the latter process is less common.[1−7] In this context, suitable multidentate ligands incorporating both phenyl and thioether functions are good candidates for providing organothiolates of noble metals via C−H and C−S bond cleavages, respectively. In pursuing our search for alkyl 2-(phenylazo)-phenyl thioether **1**, a typical ligand of this kind, we found that no metal-assisted S-dealkylation occurred with noble metal halides and only chelation modes of types **2** and **3** (Scheme 1) are cited in the literature.[5] Great attention has been paid to metal-assisted C−S bond activation from the standpoint of synthetic, catalytic, bioinorganic, and theoretical chemistry.[1−4] Interestingly, such S-dealkylation strategy (chelation mode **4**) has indeed materialized successfully with $RhCl_3 \cdot 3H_2O$ in the presence of excess PPh_3, affording organorhodium(III) thiolato complexes. Recently, rhodium thiolato and organorhodium compounds have been found to exhibit various bioactivities, including anticancer activity.[8]

* To whom correspondence should be addressed. E-mail: kpramanik@hotmail.com.
† Jadavpur University.
‡ Indian Institute of Science.
§ Université de Neuchâtel.

(1) *Transition Metal Sulfur Chemistry*; Stiefel, E. I., Matsumoto, K., Eds.; ACS Symposium Series 653; American Chemical Society: Washington, DC, 1996.

10.1021/ic7016006 CCC: $40.75
Published on Web 12/28/2007

Scheme 1. Alkyl 2-(Phenylazo)phenyl Thioether and Its Different Chelation Modes with Noble Metals

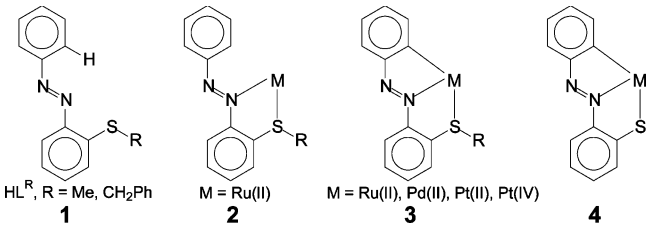

Moreover, interest in the polymetallic complexes arises from the possible "cooperative effects".[1] The self-assembly process appears as rational means to construct metallo supramolecular architectures. In rhodium thiolato chemistry, it has been recognized that the high nucleophilicity of coordinated thiolato function may furnish S-bridged polynuclear structures with other metal centers.[9] It is now of interest to stabilize and isolate the intermediate mononuclear rhodium thiolato compounds as well as to explore their chemistry during di- and polymerization processes. To the best of our knowledge, only a few instances are reported where mononuclear rhodium thiolato precursors are isolated, which ultimately afford S-bridged self-assembled products in due course of the reaction.[10,11] It is worth noting that the aforesaid precursors contain η^5-Cp ligation, and these examples of monomers can be rationalized on the basis of the coordinated Cp ligand.[12] It is now of significance to isolate and study monomeric intermediates without Cp ligand. Here we demonstrate the convenient synthesis and characterization of electronically and coordinatively saturated cyclometalated rhodium(III) thiolato complex **5** and its spontaneous self-association in solution, which has led to the isolation of an isomeric pair of dimers *anti*-**7** and *syn*-**8**. Significantly, both stacking and CH/π interactions of aryl rings with chelate rings were observed.[13] In this perspective, an account of intramolecular stacking interaction between two chelate rings in dinuclear complexes (not joined by direct metal−metal bond) reveals another structural evidence of the noncovalent interaction. In this work, the availability of the isomeric dimers **7** and **8** provides an opportunity to scrutinize the presence of noncovalent intramolecular *metallochelate*−*metallochelate* interaction.

In addition, the high nucleophilicity of the nonbridged S atom of **5** vis-à-vis high electron density on the thiolato group has been reflected in the electrochemical oxidation of rhodium sulfur compounds.[14] Redox chemistry of the afore-

(2) (a) Santra, B. K.; Lahiri, G. K. *J. Chem. Soc., Dalton Trans.* **1998**, 1613−1618. (b) Giner-Planas, J.; Marumo, T.; Ichikawa, Y.; Hirano, M.; Komiya, S. *J. Chem. Soc., Dalton Trans.* **2000**, 2613−2625. (c) Komiya, S.; Hirano, M. *J. Chem. Soc., Dalton Trans.* **2003**, 1439−1453. (d) Furuya, M.; Tsutsuminai, S.; Nagasawa, H.; Komine, N.; Hirano, M.; Komiya, S. *Chem. Commun.* **2003**, 2046−2047. (e) Chehata, A.; Oviedo, A.; Arévalo, A.; Bernès, S.; García, J. J. *Organometallics* **2003**, *22*, 1585−1587. (f) Rauchfuss, T. B. *Inorg. Chem.* **2004**, *43*, 14−26. (g) Shimizu, D.; Takeda, N.; Tokitoh, N. *Chem. Commun.* **2006**, 177−179. (h) Goj, L. A.; Lail, M.; Pittard, K. A.; Riley, K. C.; Gunnoe, T. B.; Petersen, J. L. *Chem. Commun.* **2006**, 982−984. (i) Siedle, G.; Kersting, B. *J. Chem. Soc., Dalton Trans.* **2006**, 2114−2126. (j) Helmstedt, U.; Lönnecke, P.; Hey-Hawkins, E. *Inorg. Chem.* **2006**, *45*, 10300−10308. (k) Hassan, M. R.; Kabir, S. E.; Nicholson, B. K.; Nordlander, E.; Uddin, M. N. *Organometallics* **2007**, *26*, 4627−4233.

(3) (a) Osakada, K.; Matsumoto, K.; Yamamoto, T.; Yamamoto, A. *Organometallics* **1985**, *4*, 857−862. (b) Bianchini, C.; Meli, A. *Acc. Chem. Res.* **1998**, *31*, 109−116. (c) Angelici, R. J. *Organometallics* **2001**, *20*, 1259−1275. (d) Giner-Planas, J.; Prim, D.; Rose-Munch, F.; Rose, E.; Thouvenot, R.; Vaissermann, J. *Organometallics* **2002**, *21*, 4385−4389. (e) Bianchini, C.; Meli, A.; Vizza, F. *J. Organomet. Chem.* **2004**, *689*, 4277−4290. (f) Jones, W. D. *Inorg. Chem.* **2005**, *44*, 4475−4484.

(4) (a) Mullen, G. E. D.; Fässler, T. F.; Went, M. J.; Howland, K.; Stein, B.; Blower, P. J. *J. Chem. Soc., Dalton Trans.* **1999**, 3759−3766. (b) Maresca, O.; Maseras, F.; Lledós, A. *New J. Chem.* **2004**, *28*, 625−630. (c) Magistrato, A.; Maurer, P.; Fässler, T.; Rothlisberger, U. *J. Phys. Chem. A* **2004**, *108*, 2008−2013.

(5) (a) Mahapatra, A. K.; Dutta, S.; Goswami, S.; Mukherjee, M.; Mukherjee, A. K.; Chakravorty, A. *Inorg. Chem.* **1986**, *25*, 1715−1721. (b) Mahapatra, A. K.; Bandyopadhyay, D.; Bandyopadhyay, P.; Chakravorty, A. *Inorg. Chem.* **1986**, *25*, 2214−2221. (c) Chattopadhyay, S.; Sinha, C.; Basu, P.; Chakravorty, A. *Organometallics* **1991**, *10*, 1135−1139.

(6) (a) Gerisch, M.; Krumper, J. R.; Bergman, R. G.; Tilley, T. D. *Organometallics* **2003**, *22*, 47−48. (b) Rybtchinski, B.; Cohen, R.; Ben-David, Y. J.; Martin, M. L.; Milstein, D. *J. Am. Chem. Soc.* **2003**, *125*, 11041−11050. (c) Krumper, J. R.; Gerisch, M.; Magistrato, A.; Rothlisberger, U.; Bergman, R. G.; Tiley, T. D. *J. Am. Chem. Soc.* **2004**, *126*, 12492−12502. (d) Panda, M.; Das, C.; Lee, G.-H.; Peng, S.-M.; Goswami, S. *J. Chem. Soc., Dalton Trans.* **2004**, 2655−2661. (e) Frech, C. M.; Ben-David, Y.; Weiner, L.; Milstein, D. *J. Am. Chem. Soc.* **2006**, *128*, 7128−7129. (f) Ben-Ari, E.; Cohen, R.; Gandelman, M.; Shimon, L. J. W.; Martin, J. M. L.; Milstein, D. *Organometallics* **2006**, *25*, 3190−3210.

(7) (a) Hoare, R. J.; Mills, O. S. *J. Chem. Soc., Dalton Trans.* **1972**, 2141−2145. (b) Bruce, M. I.; Humphrey, P. A.; Skelton, B. W.; White, A. H. *J. Organomet. Chem.* **1989**, *361*, 369−390. (c) Aulwurm, U. R.; Knoch, F.; Kisch, H. *Z. Kristallogr. New Cryst. Struct.* **1997**, *212*, 179−180. (d) Huang, L.-Y.; Aulwurm, U. R.; Heinemann, F. W.; Knoch, F.; Kisch, H. *Chem.−Eur. J.* **1998**, *4*, 1641−1646. (e) Dutta, S.; Peng, S.-M.; Bhattacharya, S. *J. Chem. Soc., Dalton Trans.* **2000**, 4623−4627. (f) Pratihar, J. L.; Maiti, N.; Chattopadhyay, S. *Inorg. Chem.* **2005**, *44*, 6111−6114. (g) Pratihar, J. L.; Patra, D.; Chattopadhyay, S. *J. Organomet. Chem.* **2005**, *690*, 4816−4821.

(8) (a) Sorasaenee, K.; Galán-Mascarós, J. R.; Dunbar, K. R. *Inorg. Chem.* **2002**, *41*, 433−436. (b) Sorasaenee, K.; Galán-Mascarós, J. R.; Dunbar, K. R. *Inorg. Chem.* **2003**, *42*, 661−663. (c) Dorcier, A.; Ang, W. H.; Bolaño, S.; Gonsalvi, L.; Juillerat-Jeannerat, L.; Laurenczy, G.; Peruzzini, M.; Phillips, A. D.; Zanobini, F.; Dyson, P. J. *Organometallics* **2006**, *25*, 4090−4096.

(9) (a) Yamanari, K.; Fukuda, I.; Yamamoto, S.; Kushi, Y.; Fuyuhiro, A.; Kubota, N.; Kukuo, T.; Arakawa, R. *J. Chem. Soc., Dalton Trans.* **2000**, 2131−2136. (b) Hirotsu, M.; Kobayashi, A.; Yoshimura, T.; Konno, T. *J. Chem. Soc., Dalton Trans.* **2002**, 878−884. (c) Casado, M. A.; Pérez-Torrente, J. J.; Ciriano, M. A.; Lahoz, F. J.; Oro, L. A. *Inorg. Chem.* **2004**, *43*, 1558−1567. (d) Chikamoto, Y.; Kawamoto, T.; Igashira-Kamiyama, A.; Konno, T. *Inorg. Chem.* **2005**, *44*, 1601−1610. (e) Hirata, K.; Suzuki, T.; Noya, A.; Takei I.; Hidai, M. *Chem. Commun.* **2005**, 3718−3720.

(10) Eighteen-electron monomeric precursors coordinated with labile water molecule: (a) reference 9a. (b) Yamanari, K.; Ito, R.; Yamamoto, S.; Konno, T.; Fuyuhiro, A.; Fujioka, K.; Arakawa, R. *Inorg. Chem.* **2002**, *41*, 6824−6830.

(11) Sixteen-electron monomeric precursors: (a) Jones, W. D.; Chin, R. M. *J. Am. Chem. Soc.* **1992**, *114*, 9851−9858.

(12) Rauchfuss, T. B.; Roundhill, D. M. *J. Am. Chem. Soc.* **1975**, *97*, 3386−3392.

(13) (a) Castiñeiras, A.; Sicilia-Zafra, A. G.; González-Pérez, J. M.; Choquesillo-Lazarte, D.; Niclós-Gutiérrez, J. *Inorg. Chem.* **2002**, *41*, 6956−6958. (b) Tomić, Z. D.; Novaković, S. B.; Zarić, S. D. *Eur. J. Inorg. Chem.* **2004**, 2215−2218. (c) Jiang, Y.; Xi, C.; Liu, Y.; Niclós-Gutiérrez, J.; Choquesillo-Lazarte, D. *Eur. J. Inorg. Chem.* **2005**, 1585−1588. (d) Yang, X.-J.; Drepper, F.; Wu, B.; Sun, W.-H.; Haehnel, W.; Janiak, C. *J. Chem. Soc., Dalton Trans.* **2005**, 256−267. (e) Milčič, M. K.; Medaković, V. B.; Sredojević, D. N.; Juranić, N. O.; Zarić, S. D. *Inorg. Chem.* **2006**, *45*, 4755−4763.

(14) (a) Yamada, Y.; Uchida, M.; Miyashita, Y.; Fujisawa, K.; Konno, T.; Okamoto, K *Bull. Chem. Soc. Jpn.* **2000**, *73*, 913−922. (b) Chohan, B. S.; Shoner, S. C.; Kovacs, J. A.; Maroney, M. J. *Inorg. Chem.* **2004**, *43*, 7726−7734. (c) González-Duarte, P.; Lledós, A.; Mas-Ballesté, R. *Eur. J. Inorg. Chem.* **2004**, 3585−3599. (d) Mas-Ballesté, R.; Capdevila, M.; González-Duarte, P.; Hamidi, M.; Lledós, A.; Mégret, C.; Montauzon, D. *J. Chem. Soc., Dalton Trans.* **2004**, 706−712.

said **5**−**8** compounds is scrutinized, revealing the formation of rhodium-bound thiyl radical in the case of **5**.[15]

Experimental Section

Materials. The chemicals used were purchased from the following sources: 2-aminothiophenol, triphenylphosphine, triphenylarsine, and phenyl sulfide from Aldrich Chemical Co., and $RhCl_3 \cdot 3H_2O$ from Arora Matthey Limited. All solvents were used as received.

Physical Measurements. The elemental analyses (C, H, N) were performed with a PerkinElmer model 2400 series II elemental analyzer. IR spectra were recorded on a PerkinElmer L-0100 spectrometer. The electronic spectra in dichloromethane solution were obtained using a PerkinElmer Lambda 25 spectrophotometer with a solute concentration of about 10^{-3} M. ^{1}H NMR spectral measurements were carried out on a Bruker av FT 300 MHz spectrometer with TMS as an internal reference. ^{31}P NMR spectral measurements were carried out on a Bruker AMX 500 spectrometer operating at 202.42 MHz. The electrospray ionization mass spectra (EI-MS positive) were measured in acetonitrile on a Micromass Qtof YA263 mass spectrometer. GC analysis of the solution was performed on a PerkinElmer Clarus 500 gas chromatograph equipped with a 30-m (0.25 mm i.d., 0.25-μm film thickness) ELITE 5MS column. Carrier gas He, $T1 = 40$ °C, initial isotherm time = 2 min, heating rate = 8, $T_{final} = 300$ °C, final isotherm time = 5, flow = 1 mL/min. The mass spectrometry data were collected after electron ionization at 70 eV. GC/MS analysis was performed on a PerkinElmer Clarus 500 GC/MS apparatus. X-ray intensity data for compounds **5** and **7** were measured at 293 (2) K on a Bruker AXS SMART APEX CCD diffractometer (Mo Kα, $\lambda = 0.71073$ Å). Metal atoms were located by direct methods, and the rest of the non-hydrogen atoms emerged from successive Fourier synthesis. The structures were refined by full-matrix least-squares procedures on F^2. All non-hydrogen atoms were refined anisotropically. All the hydrogen atoms were included in calculated positions for compound **5**, while those of **7** were located from difference maps and refined isotropically. X-ray intensity data for compounds **6b** and **8** were measured at 153(2) K on a Stoe Mark II-Image plate diffraction system[16] equipped with a two-circle goniometer and using Mo Kα ($\lambda = 0.71073$ Å) graphite monochromatic radiation. Image plate distance 135 mm. Metal atoms were located and solved by direct methods using the program SHELXS-97.[17] The refinement and all further calculations were carried out using SHELXL-97.[18] The hydrogen atoms were included in calculated positions and treated as riding atoms using SHELXL default parameters. Calculations were performed using the SHELXTL v5.03 program package.[19] Thermal ellipsoids were drawn at the 35% probability level. Molecular structure plots were drawn using ORTEP.[20] Electrochemical measurements were carried out at 27 °C with VersaStat II Princeton Applied Research potentiostat/galvanostat under argon. The cell contained a Pt working electrode and a Pt wire auxiliary electrode. Tetraethylammnium perclorate (NEt_4ClO_4) was used as a supporting electrolyte, and the potentials were referenced to the Ag/AgCl electrode without junction correction. Coulometric oxidation was performed at a constant potential of 1.0 V vs Ag/AgCl at 300 K in 1:1 CH_2Cl_2/CH_3CN in the presence of NEt_4ClO_4 under argon. EPR spectrum was recorded on a Varian E-109C X-band spectrometer. Magnetic susceptibilities were measured on a PAR-155 vibrating-sample magnetometer.

Computational Study. Ground-state electronic structure calculations of the organosulfur complexes using the X-ray coordinate were carried out by density functional theory (DFT)[21] method employing the Gaussian 03 (G03) program.[22] The functional used throughout the study was the B3LYP, consisting of a nonlocal hybrid exchange functional as defined by Becke's three-parameter equation[23] and nonlocal Lee−Yang−Parr correlation functional.[24] The basis set used for all non-metal atoms except hydrogen was 6-31G(d) and 6-31G for hydrogen. LANL2DZ valance and effective core potential functions were used for rhodium.

Syntheses of Ligands. (1). HL^R (R = Me, CH_2Ph) was synthesized following the methods previously described.[25]

Syntheses of Compounds. $[Rh(L)Cl(PPh_3)_2]$ (5). A mixture of **1** (R = CH_2Ph) (118 mg, 0.388 mmol), $RhCl_3 \cdot 3H_2O$ (100 mg, 0.380 mmol), and triphenylphosphine (1.0 g, 3.816 mmol) in ethanolic (50 mL) solution was heated to reflux for 16 h until a dark green crystalline solid was precipitated. The green mass was filtered, washed with ethanol, and dried under reduced pressure. Upon chromatographic purification of the solid on neutral silica gel with 1:3 hexane/benzene mixture as eluent, green **5** was obtained. Yield (41%). An analogous reaction was made with **1** (R = Me). Yield (39%). Anal. Calcd for $C_{48}H_{38}ClN_2P_2RhS$: C, 65.87; H, 4.38; N, 3.20. Found: C, 65.69; H, 4.32; N, 3.26%. UV−vis spectra (CH_2Cl_2): λ_{max}, nm (ϵ dm^{-3} mol^{-1} cm^{-1}): 711 (3600). IR (KBr disk, cm^{-1}): 1393 (ν_{NN}), 743, 693 and 518 (ν_{RhP}). ^{1}H NMR (300 MHz, $CDCl_3$): δ 7.612 (d) 7.542−7.486 (m), 7.436 (d), 7.198−7.056 (m), 6.872 (t), 6.697 (d), 6.556−6.460 (m), 6.377 (d), 6.087 (t); ^{31}P NMR ($CDCl_3$): δ 16.87 (d, $^1J_{Rh-P} = 97.6$ Hz). HRMS (EI) calcd for $C_{48}H_{38}ClN_2P_2RhS$ (M^+) 874.0938, found (m/z) 874.0875.

$[Rh(L^R)Cl_2(PPh_3)]$ (6). To an ethanolic (50 mL) solution of **1** (R = CH_2Ph) (116 mg, 0.382 mmol) and $RhCl_3 \cdot 3H_2O$ (100 mg,

(15) (a) Kimura, S.; Bill, E.; Bothe, E.; Weyhermuller, T.; Wieghardt, K. *J. Am. Chem. Soc.* **2001**, *123*, 6025−6039. (b) Journaux, Y.; Glaser, T.; Steinfeld, G.; Lozana, V.; Kersting B. *J. Chem. Soc., Dalton Trans.* **2006**, 1738−1748. (c) McDonough, J. E.; Weir, J. J.; Sukcharoenphon, K.; Hoff, C. D.; Kryatova, O. P.; Rybak-Akimova, E. V.; Scott, B. L.; Kubas, G. J.; Mendiratta, A.; Cummins, C. C. *J. Am. Chem. Soc.* **2006**, *128*, 10295−10303. (d) Grapperhaus, C. A.; Venna, K. B.; Mashuta, M. S. *Inorg. Chem.* **2007**, *46*, 8044−8050.

(16) *X-Area V1.17 and X-RED32 V1.04 Software*; Stoe & Cie: Darmstadt, Germany, 2002.

(17) Sheldrick, G. M. *SHELXS-97, Program for Crystal Structure Solution*; University of Göttingen: Göttingen, Germany, 1997.

(18) Sheldrick, G. M. *SHELXL-97, Program for Refining X-ray Crystal Structures*; University of Göttingen: Göttingen, Germany, 1997.

(19) Sheldrick, G. M. *SHELXTL*, version 5.03; Siemens Analytical Instruments: Madison, WI, 1994.

(20) Johnson, C. K. *ORTEP*; Report ORNL-5138; Oak Ridge National Laboratory: Oak Ridge, TN, 1976.

(21) Parr, R. G.; Yang, W. *Density functional theory of atoms and molecules*; Oxford University Press: New York, 1989.

(22) Frisch, M. J.; Trucks, G. W.; Schlegel, H. B.; Scuseria, G. E.; Robb, M. A.; Cheeseman, J. R.; Montgomery, J. A., Jr.; Vreven, T.; Kudin, K. N.; Burant, J. C.; Millam, J. M.; Iyengar, S. S.; Tomasi, J.; Barone, V.; Mennucci, B.; Cossi, M.; Scalmani, G.; Rega, N.; Petersson, G. A.; Nakatsuji, H.; Hada, M.; Ehara, M.; Toyota, K.; Fukuda, R.; Hasegawa, J.; Ishida, M.; Nakajima, T.; Honda, Y.; Kitao, O.; Nakai, H.; Klene, M.; Li, X.; Knox, J. E.; Hratchian, H. P.; Cross, J. B.; Bakken, V.; Adamo, C.; Jaramillo, J.; Gomperts, R.; Stratmann, R. E.; Yazyev, O.; Austin, A. J.; Cammi, R.; Pomelli, C.; Ochterski, J. W.; Ayala, P. Y.; Morokuma, K.; Voth, G. A.; Salvador, P.; Dannenberg, J. J.; Zakrzewski, V. G.; Dapprich, S.; Daniels, A. D.; Strain, M. C.; Farkas, O.; Malick, D. K.; Rabuck, A. D.; Raghavachari, K.; Foresman, J. B.; Ortiz, J. V.; Cui, Q.; Baboul, A. G.; Clifford, S.; Cioslowski, J.; Stefanov, B. B.; Liu, G.; Liashenko, A.; Piskorz, P.; Komaromi, I.; Martin, R. L.; Fox, D. J.; Keith, T.; Al-Laham, M. A.; Peng, C. Y.; Nanayakkara, A.; Challacombe, M.; Gill, P. M. W.; Johnson, B.; Chen, W.; Wong, M. W.; Gonzalez, C.; Pople, J. A. *Gaussian 03*, revision C.02; Gaussian, Inc.: Wallingford, CT, 2004.

(23) Becke, A. D. *J. Chem. Phys*. **1993**, *98*, 5648−5652.

(24) Lee, C.; Yang, W.; Parr, R. G. *Phys. Rev. B* **1998**, *37*, 785−789.

(25) Shriner, R. L.; Struck, H. C.; Jorison, W. J. *J. Am. Chem. Soc.* **1930**, *52*, 2060−2069. (b) Burawoy, A.; Vellins, C. E. *J. Chem. Soc.* **1954**, 90−95. (c) Livingstone, S. E. *J. Chem. Soc.* **1956**, 437−440.

0.380 mmol), triphenylphosphine (102 mg, 0.389 mmol) was added and heated to reflux for 4 h until a dark orange solution was obtained. The resulting solution was evaporated to dryness. Upon chromatographic purification of the solid on neutral silica gel with 1:8 acetonitrile/benzene mixture as eluent, orange **6b** was obtained. Yield (62%). An analogous reaction was made with **1** (R = Me). Yield (58%). For compound **6b**: Anal. Calcd for $C_{37}H_{30}Cl_2N_2PRhS$: C, 60.09; H, 4.08; N, 3.79. Found: C, 60.58; H, 4.29; N, 3.65%. UV−vis spectra (CH_2Cl_2): λ_{max}, nm (ϵ dm^{-3} mol^{-1} cm^{-1}): 470 (2500). IR (KBr disk, cm^{-1}): 1411 (ν_{NN}), 696 and 528 (ν_{RhP}). ^1H NMR (300 MHz, $CDCl_3$): δ 8.107 (d), 8.033 (d), 7.689 (d), 7.481−7.035 (m), 5.556 (d), 4.624 (d); ^{31}P NMR ($CDCl_3$): δ 22.21 (d, $^1J_{Rh-P}$ = 118.9 Hz). For compound **6a**: Anal. Calcd for $C_{31}H_{26}Cl_2N_2PRhS$: C, 56.12; H, 3.95; N, 4.22. Found: C, 55.79; H, 4.14; N, 4.14%. UV−vis spectra (CH_2Cl_2): λ_{max}, nm (ϵ dm^{-3} mol^{-1} cm^{-1}): 471 (2100). IR (KBr disk, cm^{-1}): 1416 (ν_{NN}), 696, 535 (ν_{RhP}). ^1H NMR (300 MHz, $CDCl_3$): δ 8.121 (d), 8.018 (d), 7.662 (d), 7.528−7.082 (m), 2.175 (s); ^{31}P NMR ($CDCl_3$): δ 21.86 (d, $^1J_{Rh-P}$ = 117.1 Hz).

Conversion of 6 to 5. 6a (45 mg, 0.068 mmol) and triphenylphosphine (144 mg, 0.551 mmol) were dissolved in ethanol (30 mL), and the mixture was refluxed for 10 h. During this time, green precipitate of compound **5** was formed. Chromatographic purification was made by the above procedure. Yield (57%). An analogous reaction with **6b** produced **5** in 55% yield.

***anti*-[Rh(L)Cl(PPh$_3$)]$_2$ (7) and *syn*-[Rh(L)Cl(PPh$_3$)]$_2$ (8).** In a typical reaction, toluene solution (150 mL) of compound **5** (100 mg, 0.114 mmol) was refluxed for 100 h. The original green solution slowly turned dark red. Organic solvent was evaporated under reduced pressure, and the resulting dark mass was subjected to column chromatography. Compounds **8** and **7** were eluted as a brown band with benzene and red band with 1:10 acetonitrile/benzene mixture, respectively. Yield for **7** (58%) and for **8** (8%). An analogous reaction was performed at room temperature in toluene for 4 months. Then the compounds were isolated as above. Yield for **7** (55%) and for **8** (8%). For compound **7**: Anal. Calcd for $C_{60}H_{46}Cl_2N_4P_2Rh_2S_2$: C, 58.78; H, 3.78; N, 4.58. Found: C, 58.65; H, 3.84; N, 4.49%. UV−vis spectra (CH_2Cl_2): λ_{max}, nm (ϵ dm^{-3} mol^{-1} cm^{-1}): 529 (5400). IR (KBr disk, cm^{-1}): 1385 (ν_{NN}), 694 and 526 (ν_{RhP}). ^1H NMR (300 MHz, $CDCl_3$): δ 8.351 (d), 7.734 (d), 7.468−7.407 (m), 7.160−7.001 (m), 6.695−6.502 (m), 5.684 (d); ^{31}P NMR ($CDCl_3$): δ 23.52 (d, $^1J_{Rh-P}$ = 115.2 Hz). HRMS (EI) calcd for $C_{60}H_{46}Cl_2N_4P_2Rh_2S_2$ (M^+) 1224.0156, found (*m*/*z*) 1224.0077. For compound **8**: Anal. Calcd for $C_{60}H_{46}Cl_2N_4P_2Rh_2S_2$: C, 58.78; H, 3.78; N, 4.58. Found: C, 58.61; H, 3.72; N, 4.48%. UV−vis spectra (CH_2Cl_2): λ_{max} nm (ϵ dm^{-3} mol^{-1} cm^{-1}): 508 (3800). IR (KBr disk, cm^{-1}): 1388 (ν_{NN}), 694 and 522 (ν_{RhP}). ^1H NMR (300 MHz, $CDCl_3$): δ 8.178 (d), 7.660 (d), 7.273 (t), 7.153−7.039 (m), 6.991−6.940 (m), 6.827 (t); ^{31}P NMR ($CDCl_3$): δ 23.11 (d, $^1J_{Rh-P}$ = 116.6 Hz). HRMS (EI) calcd for $C_{60}H_{46}Cl_2N_4P_2Rh_2S_2$ (M^+) 1224.0156, found (*m*/*z*) 1224.0089.

Conversion of Dimers (7 and 8) to Monomer (5). Compound **7** (20 mg, 0.016 mmol) and triphenylphosphine (25 mg, 0. 095 mmol) were dissolved in toluene (5 mL), and the mixture was refluxed for 48 h. The solution turned dark green, and compound **5** was isolated by the above procedure. Yield (71%). An analogous reaction was performed with **8**. Yield (68%).

Results and Discussion

Synthesis and Spectroscopic Characterization. Treatment of an alcoholic solution of $RhCl_3 \cdot 3H_2O$ with **1** in the presence of 10-fold excess of PPh_3 under refluxing condition

Scheme 2. Syntheses and Structures of Orthometalated Rhodium(III) Thiolato **5** and Thioether **6** Compounds

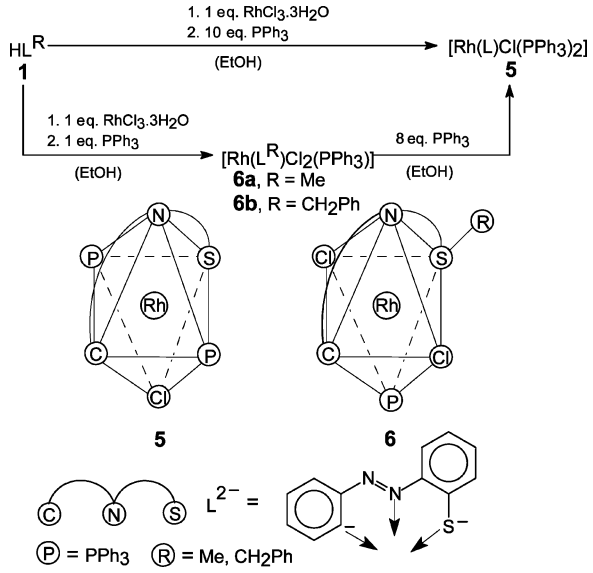

afforded an emerald solid **5** in 40% yield (Scheme 2). Both C(sp^2)−H and C(sp^3)−S bonds were cleaved in situ during the course of the synthesis. The general mechanism of formation of orthometalated azobenzene derivatives was described to proceed via initial coordination of azo-nitrogen followed by electrophilic substitution at the pendant phenyl ring.[7g,26]

It is worth noting that the C−S bond scission was not observed when reactions were performed with 1 equiv of PPh_3 relative to both **1** and $RhCl_3 \cdot 3H_2O$. In that case, orange organothioether rhodium(III) compounds **6** (chelation mode **3**) are obtained. Although the S-dealkylation is not observed with $RhCl_3$ in the absence of PPh_3, Wilkinson's catalyst, viz. [RhCl(PPh_3)$_3$], alone is competent to furnish **5** in the analogous conditions in low yield. Interestingly, the thioether functions of **6** are converted to thiolato group in presence of excess PPh_3 to afford organothiolato rhodium **5** (Scheme 2). Although the oxidation states of rhodium remain the same in both the starting material and organothiolato product, we speculate it passes through an intermediate rhodium(II) species that could possibly be involved in the C−S bond cleavage process. However, attempts to observe any Rh(II) intermediates along the reaction pathway were unsuccessful. Interestingly, use of less π-acidic SPh_2 and $AsPh_3$ instead of PPh_3 appears ineffective for such bond cleavage, indicating that the C−S bond activation is sensitive to the π-acidity of the added coligand. The reason behind this observation possibly lies in the stabilization of the proposed Rh(II) intermediate. Tertiary phosphine ligands have a strong stabilizing effect on transition-metal complexes in low oxidation states owing to their π-acceptance nature.[27,28] The stability of such complexes has been exploited in various

(26) (a) Aulwurm, U. R.; Melchinger, J. U.; Kisch, H. *Organometallics* **1995**, *14*, 3385−3395. (b) Lersch, M.; Tilset, M. *Chem. Rev.* **2005**, *105*, 2471−2526. (c) Dupont, J.; Consorti, C. S.; Spencer, J. *Chem. Rev.* **2005**, *105*, 2527−2571. (d) Patra, D.; Pratihar, J.; Shee, B.; Pattanayak, P.; Chattopadhyay, S. *Polyhedron* **2006**, *25*, 2637−2642.

(27) Al-Jeboori, M. J.; Dilworth, J. R.; Zheng, Y. *J. Chem. Soc., Dalton Trans.* **1998**, 3215−3218.

Scheme 3. Suggested Mechanism of C−S Cleavage

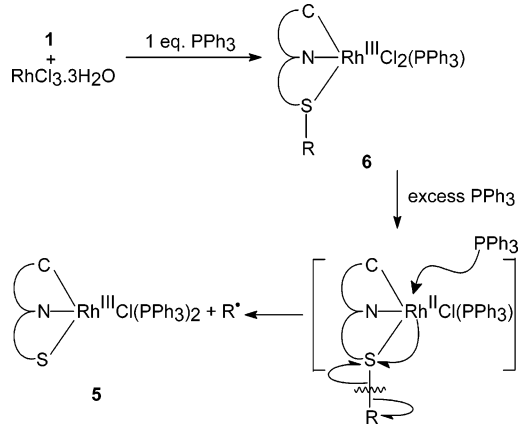

carbon−heteroatom bond activation processes via oxidative addition.[2b−d,29] This strategy may be utilized as a useful tool for a variety of C−heteroatom bond-breaking processes. Moreover, ample precedent exists for internal oxidative addition of one such C−S bond of coordinated thiophene to Rh(III) where reductive cleavage of C−heteroatom bond occurs.[3b−f] In our case, selective C−S bond viz. C(sp^3)−S is cleaved consistent with the bond strength order (C(sp^3)−S < C(sp^2)−S). The reductive cleavage of C(sp^3)−S bond of coordinated thioether moiety has been explored as an attractive route to functional ligands and new materials.

A plausible mechanism of the C−S cleavage reaction process is proposed as shown in Scheme 3.[30] We anticipate that, after initial coordination of HL^R with Rh(III), the resultant organothioether rhodium(III) compounds **6** get reduced in the presence of excess phosphine to the intermediate organothioether rhodium(II) complex. Although no low valence reaction intermediates have been observed or isolated, a rhodium(II) intermediate is a likely active species. In view of the proposed mechanism presented in Scheme 3, it is reasonable to conclude that the conversion of **6** to **5** proceeds through the intermediacy of the Rh(II) fragment [Rh(L^R)Cl(PPh_3)] (electron-rich d^7 center), which is active toward the one-electron reduction of the coordinated S−C(sp^3) bond of thioether group from L^R (via electron donation into the C−S σ^* antibonding orbital)[4c,31] and causes reductive cleavage of pendant S−C(alkyl) bond with concomitant extrusion of alkyl radical (R•). To obtain support for this proposed mechanism, GC/MS analysis (Figure S1 in the Supporting Information) of the reaction mixture was performed for HL^{CH_2Ph}.[32] The reactive alkyl radical is transformed to various products, namely R−H, R−Cl, R−OEt, and R−R. The chromatogram is consistent with reductive cleavage by single-electron transfer (SET) mechanism since the products (comparable yield of toluene, benzyl chloride, and ethyl benzyl ether and a little bibenzyl) appear to be derived from radical species.[33,34]

Scheme 4. Syntheses and Structures of Organorhodium(III) Thiolato Dimers

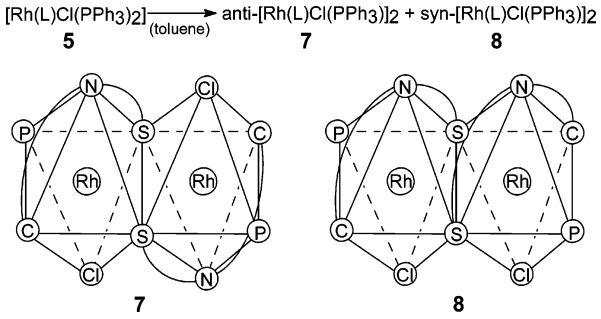

The mononuclear thiolato complex was found to be indefinitely stable in the solid state. Surprisingly, electronically and coordinatively saturated complex **5** appeared to be unstable in solvents such as toluene, dichloromethane, and so forth at ambient conditions and undergoes dimerization. Nonetheless, spectral study ensures the substantial stability of **5** (t_2^6, substitutionally inert)[28] in solution. It slowly self-dimerized via dissociation of one coordinated PPh_3 ligand in solution to thiolato-bridged magenta **7** and brown **8** dimers in approximately 7:1 ratio (Scheme 4). Interestingly, upon boiling the concentrated toluene solution of respective dimer with 6 equiv of PPh_3, mononuclear **5** was regenerated. Phosphine-mediated mononuclear-dinuclear interconversion occurs presumably via a 16-electron five-coordinated intermediate [Rh^{III}(L)Cl(PPh_3)].

All three organorhodium(III) thiolates were isolated as both air- and moisture-stable solids and characterized both in solution by UV−vis, NMR (^{1}H and ^{31}P), and mass spectroscopies and in the solid state by IR, susceptibility measurement, and single-crystal X-ray diffraction studies. The thioether complexes **6a** and **6b** were analogously characterized, and X-ray structure of one representative compound was determined. Additionally, ligand redox behavior of the organosulfur compounds was scrutinized by

(28) Cotton, F. A.; Wilkinson, G.; Murrilo, C. A.; Bochmann, M. *Advanced Inorganic Chemistry*, 6th ed.; Wiley-Interscience: New York, 1999.
(29) (a) Ohta, T.; Michibata, T.; Yamada, K.; Omori, R.; Furukawa, I. *Chem. Commun.* **2003**, 1192−1193. (b) Li, M.; Ellern, A.; Espenson, J. H. *Angew. Chem., Int. Ed.* **2004**, *43*, 5837−5839. (c) Li, M.; Ellern, A.; Espenson, J. H. *J. Am. Chem. Soc.* **2005**, *127*, 10436−10447.
(30) We are thankful for the helpful mechanistic discussion with one of the reviewers.
(31) (a) Jones, W. D.; Dong, L. *J. Am. Chem. Soc.* **1991**, *113*, 559−564. (b) Dong, L.; Duckett, S. B.; Ohman, K. F.; Jones, W. D. *J. Am. Chem. Soc.* **1992**, *114*, 151−160.
(32) We could not perform GC/MS analysis in the case of HL^{Me} since the products derived from methyl radical are highly volatile and were unable to arrest during the synthesis of organothiolato compound **5**.
(33) While open questions remain about the preferred pathway for C−S bond cleavage of coordinated thioether moiety of **6**, the observed products from the GC/MS study do provide some insight into the mechanism of cleavage for these organothioether compounds. Formation of R^+ by heterolytic cleavage is not a reasonable mechanism for the C−S bond rupture of organothioether rhodium(III) systems since the generation of R−R is rather unexpected via alkyl cation. In addition, formation of the corresponding alkane via hydride abstraction appears less likely. Alternative mechanisms include (1) two electrons reductive cleavage and the formation of R^- proceeds through the intermediacy of the Rh(I) fragment [Rh(L^R)(PPh_3)] and (2) an initial formal reduction at the metal center to the unstable intermediate [Rh^{II}-(L^R)Cl(PPh_3)] (phosphines are well known reducing agent) followed by SET to the S−C(alkyl) σ^* antibonding orbital with the release of R• as cleavage product. Since the observed products derived from alkyl group contain benzyl chloride and ethyl benzyl ether as well (Figure S1 in the Supporting Information), we suggest that the latter reaction pathway is most likely to be operative. The plausible radical reactions can be written as: $PhCH_2^\bullet + EtOH \rightarrow PhCH_3 + EtO^\bullet$; $EtO^\bullet + PhCH_2^\bullet \rightarrow EtOCH_2Ph$; $PhCH_2^\bullet + [Cl-Rh^{III}] \rightarrow PhCH_2Cl + [Rh^{II}]$[34]; $2PhCH_2^\bullet \rightarrow PhCH_2CH_2Ph$.
(34) Bacha, J. D.; Kochi, J. K. *J. Org. Chem.* **1968**, *33*, 83−93.

cyclic voltammetric study. The radical cation $\mathbf{5}^{\bullet+}$ complex generated by electrochemical means was characterized by EPR spectroscopy.

Infrared spectra of the complexes exhibit many sharp and strong vibrations within 1750−400 cm^{-1}. A sharp vibration observed near 1400 cm^{-1} for all the complexes is assigned to the ν_{NN}. The expected lowering of ν_{NN} values of complexes as compared with those of **1** is consistent with the Rh(III) → π^*(azo) back-bonding.[5a] Strong bands near 520 and 690 cm^{-1} are indicative of Rh−PPh_3 ligation in the complexes, while an additional intense feature at 743 cm^{-1} is observed in the case of **5**, which may be attributed to the presence of a *trans*-Rh$(PPh_3)_2$ moiety.

Thiolato and thioether complexes are soluble in both nonpolar and polar organic solvents such as benzene, toluene, dichloromethane, acetone, and so forth. Electronic spectra of all the complexes have been recorded in dichloromethane solution (Figure S2 in the Supporting Information). The mononuclear rhodium thiolato compound shows absorption near 700 nm in the visible region. The lowest energy absorptions of the organothiolato complexes in the visible region are probably due to intraligand charge-transfer transitions taking place in the three-coordinated 2-(phenylazo)-thiolate ligand and are corroborated with the nature of FMOs (vide supra).[7e] Observed hypsochromic shift of the lowest energy excitation in UV−vis spectra of **7** and **8** (529 and 508 nm, respectively) relative to that of **5** is ascribed to the weaker charge-transfer transition upon μ-SAr dimerization. The lowest energy electronic excitation of thioether complexes is shifted to higher energy (~470 nm) as compared with that of thiolato compounds, indicating that facile CT transition occurs in S-dealkylated complexes.

All the synthesized complexes gave satisfactory elemental analyses and were diamagnetic, which corresponds to the trivalent rhodium (low-spin d^6, $S = 0$) in these complexes. Absence of alkyl resonance in the ^1H NMR spectrum of **5** validates the occurrence of S-dealkylation. Alkyl proton signals of thioether compounds **6a** and **6b** appear as a singlet at δ 2.2 (SCH_3) and a pair of doublets centered at δ 5.1 (SCH_2Ph, $^1J_{HH} = 12.3$ Hz) resonances, respectively. The ^1H NMR spectra of **7** and **8** show a 1:1 relation of ligand/triphenylphosphine signals, corresponding to the thiolato-bridged dinuclear rhodium(III) hexacoordinated species with loss of one PPh_3 molecule per metal center of the parent monomer. The ^{31}P NMR spectra of the thiolato complexes containing two phosphine groups exhibit only single doublet resonances, indicating equivalent phosphine environment (i.e., trans and anti dispositions of PPh_3 groups in monomeric and dimeric complexes, respectively). The formation of dimers results in a significant deshielding (dimers $\delta \approx 23$ vs monomer $\delta \approx 17$) in the ^{31}P signals. The higher $^1J_{Rh-P}$ values of dimers by ca. 18 Hz in comparison to those of **5** are indicative of the shorter Rh−P lengths in the former compounds (vide supra). The ^{31}P signals of the thioether complexes occur near $\delta \approx 22$.

Both the NMR and MASS spectroscopic studies unequivocally established the substantial stability of cyclometalated rhodium thiolato compounds in the solution phase (Figures S3 and S4 in the Supporting Information). These attributions are consistent with the crystal structures showed in Figures 3 (compound **5**), 4(compound **6b**), and 5(compounds **7** and **8**).

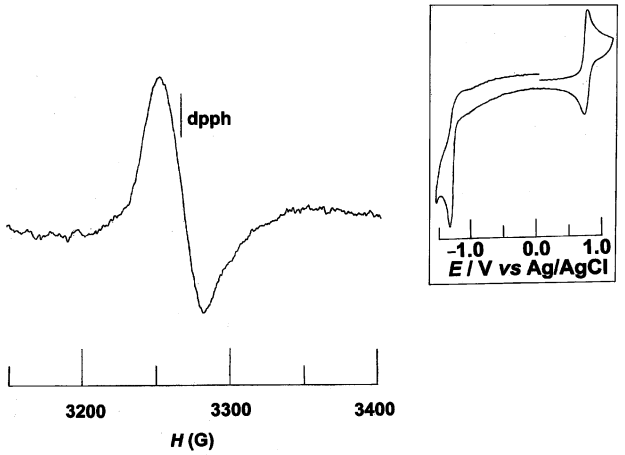

Figure 1. X-band EPR spectrum of $\mathbf{5}^{\bullet+}$ in CH_2Cl_2 at 300 K. Instrument settings: microwave frequency, 9.1 GHz; microwave power, 28 dB; modulation frequency, 100 kHz. Voltammogram of **5** in 1:1 CH_2Cl_2/CH_3CN at 50 mV s^{-1} is shown in the inset.

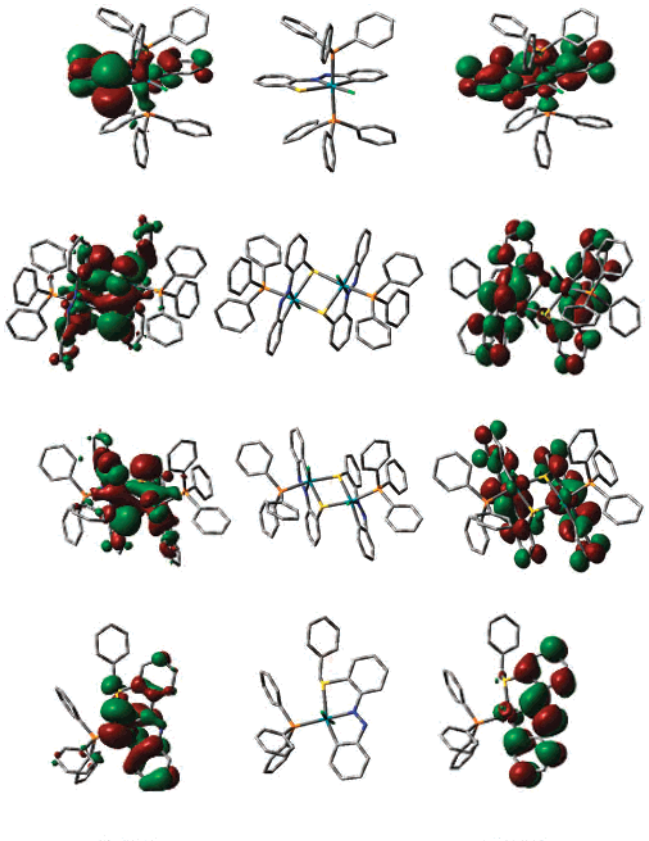

Figure 2. HOMO and LUMO of organothiolato **5** (top), **7**, **8**, and organothioether **6b** (bottom) compounds (isosurface cutoff value = 0.02). Color code for atom: gray, C; blue, N; orange, P; yellow, S; green, Cl; aquamarine, Rh.

Ligand Redox and EPR. Electron-transfer property of the organosulfur rhodium(III) complexes was studied by using cyclic voltammetry in 1:1 dichloromethane/acetonitrile solution (0.1 M NEt_4ClO_4) by using a platinum working electrode (Table 1). The reported potential is referenced to

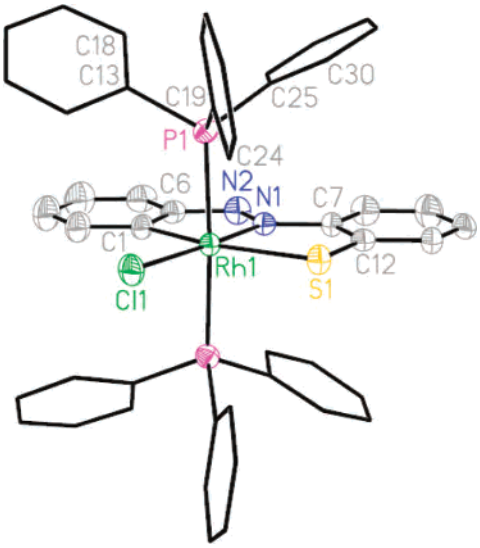

Figure 3. Molecular structure of **5**. Solvate and H atoms are omitted for clarity. Selected bond lengths (Å) and angles (deg): Rh1−C1 2.025(6), Rh1−N1 1.990(5), Rh1−Cl1 2.368(2), Rh1−P1 2.363(2), Rh1−S1 2.452-(2), N1−N2 1.280(7), C12−S1 1.761(7); N1−Rh1−S1 83.85(15), P1−Rh1−P2 174.85(9).

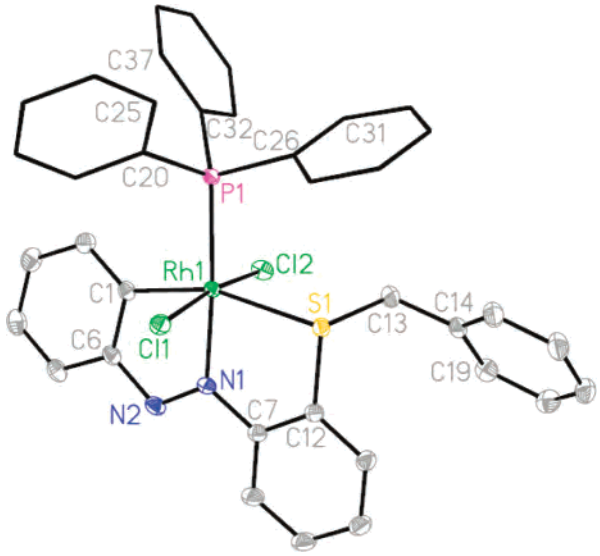

Figure 4. Molecular structure of **6b**. H atoms are omitted for clarity. Selected bond lengths (Å) and angles (deg): Rh1−C1 2.003(1), Rh1−N1 2.028(1), Rh1−Cl1 2.341(1), Rh1−Cl2 2.338(1), Rh1−P1 2.336(1), Rh1−S1 2.472(1), N1−N2 1.265(2), C12−S1 1.785(1), C13−S1 1.839(1); Cl1−Rh1−Cl2 173.22(1), N1−Rh1−S1 82.51(3), N1−Rh1−P1 174.60(3).

the Ag/AgCl electrode. The value for the ferrocenium−ferrocene couple, under our experimental conditions, was 0.52 V.

Unlike organothioether complexes, the mononuclear [Rh^{III}(L)Cl(PPh$_3$)$_2$] shows an oxidative response at $E_{1/2} = +0.82$ V vs Ag/AgCl and the voltammogram is reversible in nature, characterized by a rather small peak-to-peak separation ($\Delta E_p = E_{pa} - E_{pc}$) of 80 mV. This indicates the oxidative potential is sensitive to the nature of the metal−sulfur (thioether vs thiolato) bonding. Voltammogram of the mononuclear thiolato complex is shown in the inset of Figure 1. The one-electron nature of this oxidation has been verified by comparing its current height (i_{pa}) with that of the standard ferrocene−ferrocenium couple under identical experimental conditions. Coulometric study at 300 K confirms the oxidation to be a one-electron process and demonstrates a fully reversibile **5**/**5**$^{\bullet+}$ couple. It is very likely that this process corresponds to the oxidation of the thiophenolate sulfur atom, yielding a rhodium-bound thiyl radical (eq 1).[15]

$$[Rh^{III}(L^{-II})Cl(PPh_3)_2] - e^- \leftrightarrow [Rh^{III}(L^{-I})Cl(PPh_3)_2]^+ : E_{1/2} \qquad (1)$$

The redox noninnocence of the thiophenolate donor in the mononuclear species is supported by the EPR and theoretical studies. It should be noted that the dinuclear species **7** and **8** display a single, irreversible redox wave near $E_{pa} = +1.2$ V vs Ag/AgCl. The oxidative response can be assigned primarily to a ligand-centered redox reaction. In contrast, all the complexes show one-electron irreversible reduction waves between −1.0 and −1.5 V vs Ag/AgCl. These responses are believed to be centered on the coordinated ligand with substantial contribution of the azo moiety (Figure 2).[5a]

The fluid solution X-band EPR spectrum of **5**$^{\bullet+}$ radical cation complex generated electrochemically in the presence of NEt_4ClO_4 exhibits a single line at $g = 2.003$ with the peak-to-peak line width of 28 G (Figure 1). The isotropic and intense feature of the spectrum signifies little or no contribution of metal to the spin-bearing orbital.[15,35] We believe that the thiyl radical in the one-electron oxidized **5**$^{\bullet+}$ form is stabilized by coordination to a kinetically inert Rh^{III} (t_2^6) ion.[15b]

To gain insight into the nature of the redox orbitals, we performed DFT calculation (vide infra) on compounds **5**−**8** (Figures 2 and S5 in the Supporting Information). Calculation indicates that HOMOs of organothiolato compounds are exclusively distributed over the ligand with an appreciable contribution from the 3p AO of thiolato sulfur. The oxidative response is believed to be largely centered on the S atom of coordinated 2-(phenylazo)thiolate ligand (eq 1). It is worth noting that the absence of oxidative response for thioether complexes is nicely corroborated with the insignificant contribution of S atom in the HOMO of **6b**. In contrast, the components of LUMOs are essentially AOs of azo ligands, especially N atoms with no significant participation of S orbitals.

Ligand-centered electrochemical oxidation reveals the noninnocent nature of the thiolato coordination in mononuclear species. Thus, the high electron density on the S atom of **5** facilitates the formation of S-bridged dinuclear compounds.[9,14]

Description of the Crystal Structures. The X-ray crystal structures of **5.2CH$_2$Cl$_2$**, **6b**, **7.2CH$_2$Cl$_2$**, and **8.CH$_2$Cl$_2$** were determined to establish the geometries about the metal ions as well as the bonding modes of the L^{R-}, L^{2-}, and the coligands. Single crystals of the respective complex suitable for X-ray analysis were grown by slow diffusion of hexane into dichloromethane solution at room temperature. Experi-

(35) (a) Pramanik, K.; Shivakumar, M.; Ghosh, P.; Chakravorty, A. *Inorg. Chem.* **2000**, *39*, 195−199. (b) Pramanik, K. Ph.D. Thesis, Jadavpur University, Kolkata, India, 1997.

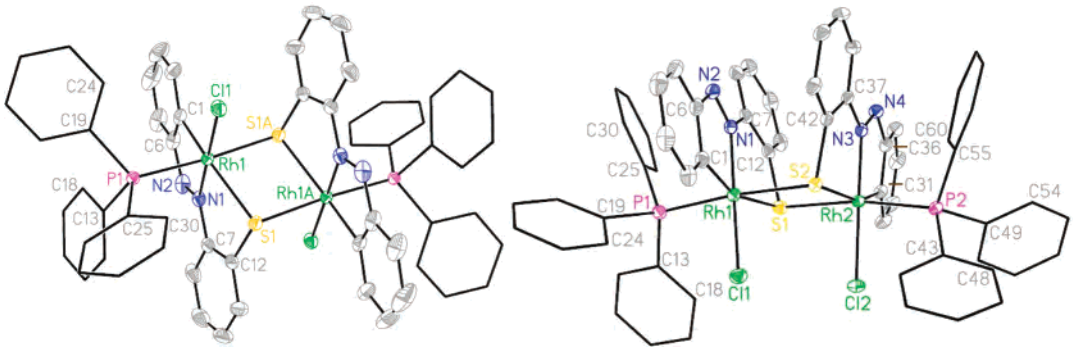

Figure 5. Molecular structure of **7** (left) and **8** (right). Solvate and H atoms are omitted for clarity. Selected bond lengths (Å) and angles (deg) of **7**: Rh1−C1 2.014(3), Rh1−N1 1.971(3), Rh1−Cl1 2.373(1), Rh1−P1 2.342(1), Rh1−S1 2.452(1), Rh1−S1A 2.478(1), N1−N2 1.274(4), C12−S1 1.776(4), Rh1···Rh1A 3.675(1), S1···S1A 3.287(2); N1−Rh1−Cl1 178.04(8), N1−Rh1−S1 83.75(9); Compound **8**: Rh1−C1 2.004(2), Rh1−N1 1.983(2), Rh1−Cl1 2.378(1), Rh1−P1 2.322(1), Rh1−S1 2.473(1), Rh1−S2 2.409(1), N1−N2 1.274(3), Rh2−C31 2.002(2), Rh2−N3 1.983(2), Rh2−Cl2 2.368(1), Rh2−P2 2.316(1), Rh2−S2 2.471(1), Rh2−S1 2.418(1), N3−N4 1.273(3), C12−S1 1.775(3), C42−S2 1.763(2), Rh1···Rh2 3.593(1), S1···S2 3.309(1); N1−Rh1−Cl1 173.59(6), N3−Rh2−Cl2 174.55(6), N1−Rh1−S1 83.11(6), N3−Rh2−S2 83.22(5).

Table 1. Electrochemical Data for **5**−**8**[a]

compound	$E_{1/2}$/V (ΔE_p/mV)
5 [Rh(L)Cl(PPh$_3$)$_2$]	−1.32,[b] +0.82(80)
6a [Rh(L^{Me})Cl$_2$(PPh$_3$)]	−1.34[b]
6b [Rh(L^{CH_2Ph})Cl$_2$(PPh$_3$)]	−1.28[b]
7 *anti*-[Rh(L)Cl(PPh$_3$)]$_2$	−1.21,[b] −1.02,[b] +1.24[c]
8 *syn*-[Rh(L)Cl(PPh$_3$)]$_2$	−1.19,[b] −1.01,[b] +1.12[c]

[a] Solute concentration ≈ 10^{-3} mol dm^{-3}; scan rate, 50 mV s^{-1}; $E_{1/2} = 0.5(E_{pa} - E_{pc})$ for reversible one-electron process, where E_{pa} and E_{pc} are the anodic and cathodic peak potentials, respectively; $\Delta E_p = E_{pa} - E_{pc}$. [b] E_{pc} value. [c] E_{pa} value.

mental crystallographic data are summarized in Table 2. Further data are available in the Supporting Information.

5.2CH$_2$Cl$_2$. The unit cell of **5** consists of [Rh(L)Cl(PPh$_3$)$_2$] neutral molecules, with dichloromethane as solvate. In this complex, the central rhodium(III) is surrounded with a distorted octahedral coordination environment by tridentate bianionic ligand (C, N, S), two *trans*-PPh$_3$, and one chloride ligands. The ligand, $[L]^{2-}$, is orthometalated and coordinates to rhodium(III) using the *ortho*-carbon C(1), azo-nitrogen N(1), and thiolato sulfur S(1) so as to form two five-membered chelates. Primary valence satisfying ligands (L^{2-} and Cl^-) and metal center lie on a crystallographic plane indicating the C_s symmetry of **5**. We wish to note here that such a coordination mode of the reference ligand via both C−H and C−S bond dissociations has not been observed previously. The bianionic ligand of type **4** is new, and rhodium(III) cyclometalates with azo function are sparse.[7]

6b. Figure 4 shows the molecular view and atom numbering scheme of a representative **6b** ($HL^R = HL^{CH_2Ph}$) complex. Crystallographic analysis of the thioether complex reveals a distorted octahedral structure with meridional C, N, S coordination of type **3** and the ligand, $[L^{CH_2Ph}]^-$, acts as a tridentate monoanionic donor. The coordination sphere of the metal atom is completed by one triphenylphosphine and two *trans*-chloride ligands. Expectedly, S1−C12 length is shorter than S1−C13 length (1.785(1) and 1.839(1) Å, respectively, C(sp^2) vs C(sp^3)). Both S1−C12 and S1−C13 bond lengths of the complex are longer by ca. 0.025 and 0.022 Å compared to the respective bonds of the free ligand (Table S1 and Figure S6 in the Supporting Information).

Several significant differences are observed between the thiolato **5** and thioether **6b** complexes, notably: (i) Rh1−S1(thioether) distance is longer by 0.02 Å than the analogous Rh1−S1(thiolato) distance, indicating enhanced bonding ability of the latter; (ii) Rh1−N1(trans to π-acid ligand PPh$_3$) length of **6b** is significantly longer (∼0.04 Å) than Rh1−N1(trans to chloride ligand) length of **5**, which is consistent with the superior overlap of the PPh$_3$ d/o* orbital with metal d orbital compared to the poorer overlap between chloride d and metal d orbitals; (iii) N1−N2 azo distances in thioether, thiolato, and free ligand HL^{CH_2Ph} (Figure S6 in the Supporting Information) are 1.265(2), 1.280(7), and 1.251(3) Å, respectively, signifying that Rh^{III}(4d) → N(azo π*) back-bonding severely impedes in presence of π-acceptor PPh$_3$ ligands in the trans position; (iv) Rh1−P1(trans to azo) length of **6b** is significantly shorter by ca. 0.03 Å than Rh1−P1(trans to PPh$_3$ ligand) length of **5** (π-acidity order: PPh$_3$ > azo); (v) Rh1−Cl(trans to chloride) average length of **6b** is significantly shorter by ca. 0.03 Å than Rh1−Cl1(trans to azo) length of **5** (trans influence order: azo > chloride); and (vi) in the structure of **5** the N, S chelate bite angle of the bianionic ligand $[L]^{2-}$, 83.85(15)°, is marginally larger than that of the monoanionic ligand $[L^{CH_2Ph}]^-$ of **6b**, 82.51(3)°.

7.2CH$_2$Cl$_2$ and 8.CH$_2$Cl$_2$. The molecules **7** and **8** are isomeric dimers and crystallize in monoclinic $C2/c$ and $P2_1/n$ space group, respectively, with Z values of 4 indicating the former contains a crystallographically imposed inversion center. The asymmetric unit contains dichloromethane as solvent of crystallization for both compounds. Crystallographic analysis reveals both are edge-shared bioctahedra consisting of a Rh$_2$S$_2$ core, in which two bridging ligands vis-à-vis Cl atoms adopt anti and syn positions, respectively. The valence electron count for Rh atoms (18 electrons per metal) and long Rh···Rh separations (Rh−Rh single bond distance, 2.4−2.9 Å)[36] rule out any metal···metal covalent interaction in the dimers. Significantly, the Rh···Rh distance of **8** is shorter by ca. 0.08 Å than that of **7**. The anti isomer has a crystallographically imposed inversion center at the midpoint of the Rh1−Rh1A vector signifying the exact planarity of the Rh$_2$S$_2$ four-membered ring, where the

(36) Cotton, F. A.; Walton, R. A. *Multiple bonds between metal atoms*, 2nd ed.; Oxford University Press: New York, 1993.

Table 2. Summarized Crystallographic Data for **5.2CH_2Cl_2**, **6b**, **7.2CH_2Cl_2**, and **8.CH_2Cl_2**

params	5.2CH_2Cl_2	6b	7.2CH_2Cl_2	8.CH_2Cl_2
empirical formula	$C_{50}H_{42}Cl_5N_2P_2RhS$	$C_{37}H_{30}Cl_2N_2PRhS$	$C_{62}H_{50}Cl_6N_4P_2Rh_2S_2$	$C_{61}H_{48}Cl_4N_4P_2Rh_2S_2$
fw	1045.02	739.47	1395.64	1310.71
T/K	293(2)	153(2)	293(2)	153(2)
cryst syst	orthorhombic	triclinic	monoclinic	monoclinic
space group	$Cmc2_1$	$P\bar{1}$	$C2/c$	$P2_1/n$
a/Å	14.995(10)	9.6036(6)	24.242(11)	11.3564(5)
b/Å	18.277(12)	11.1046(7)	0.311(5)	24.2964(8)
c/Å	17.451(11)	16.5264(10)	25.882(11)	20.4698(9)
α/deg	90.0	92.453(5)	90.0	90.0
β/deg	90.0	105.235(5)	114.169(7)	100.944(4)
γ/deg	90.0	109.209(5)	90.0	90.0
V/Å^3	4783(5)	1589.59(17)	5902(4)	5545.3(4)
Z	4	2	4	4
D_c/Mg m^{-3}	1.451	1.545	1.571	1.570
μ/mm^{-1}	0.784	0.852	1.000	0.966
cryst size/mm^3	0.40 × 0.30 × 0.20	0.30 × 0.25 × 0.20	0.35 × 0.21 × 0.16	0.32 × 0.31 × 0.08
θ/deg	1.76−24.99	2.19−29.47	1.8−25.4	1.31−25.50
measured reflns	16967	20562	21294	41222
unique reflns/R_{int}	4170/0.0245	8616/0.0215	5399/0.0301	10241/0.0319
GOF on F^2	1.119	1.028	1.122	1.029
R1,[a] wR2[b] [$I > 2\sigma(I)$]	0.0376, 0.0957	0.0217, 0.0565	0.0360, 0.0821	0.0260, 0.0621
R indices (all data) R1, wR2	0.0380, 0.0960	0.0234, 0.0573	0.0423, 0.0852	0.0358, 0.0647
largest diff. peak, hole/e Å^3	0.509 and −0.531	0.378 and −0.873	0.661 and −0.425	1.069 and −0.818

[a] $R1 = \sum|F_o| - |F_c|/\sum|F_o|$. [b] $wR2 = [\sum w(F_o^2 - F_c^2)^2/\sum w(F_o^2)^2]^{1/2}$.

corresponding ring for syn isomer slightly deviates from planarity (md 0.022 Å). Although Rh_2S_2 has been a long-standing motif in rhodium chemistry with physical data generally consistent with bisquare planar and bitetrahedral configurations, the structurally authenticated bioctahedra containing Rh_2S_2 core are scarce.[8a,37]

Metrical parameters associated with Rh−C, Rh−N, Rh−Cl, and N−N linkages in the three thiolato complexes are comparable. The Rh(III) → π^*(azo) description (vide infra) is consistent with the lengthening of N−N distance by 0.02−0.03 Å upon coordination. Slight shortening of Rh−P distances of **7** by ca. 0.02 Å as compared to that of **5** is corroborated with the weaker trans influence of the bridging thiolato than PPh_3 ligand. Additional shortening of Rh−P lengths by 0.02−0.03 Å of **8** is caused by the $\pi-\pi$ stacking interaction between phenyl(thiolato) and phenyl(PPh_3) rings (Table S2 in the Supporting Information).[38] The syn isomer differs appreciably in the orientation of the phenyl rings of PPh_3 groups (Figures S7 and S8 in the Supporting Information).

Each μ-SAr group unsymmetrically bridges the two Rh centers in both dimers. The Rh1−S1 distance of the anti isomer remains practically unaltered with that of **5**, while the Rh1−S1A distance is elongated by 0.026 Å. In contrast, anomalous shortening of the Rh1−S2 distance of the syn isomer by ca. 0.06 Å than both Rh1−S1 and Rh1−S1A distances of **8** and **7**, respectively, may plausibly be explained by invoking the "metal chelate ring−ring" interaction. Structural study of **8** provides the significance of intramolecular noncovalent "*metallochelate−metallochelate*" and "phenyl−phenyl" stacking interactions (Table S2 in the Supporting Information) toward the stabilization of sterically encumbered syn isomer (Figures S7 and S8 in the Supporting Information). It is worth noting that the stacking tendencies diverge significantly in the two isomeric forms. In consequence, the sterically hindered isomer is also formed during the self-association process since L^{2-} exhibits face-selective dimerization as well.

Conclusions

The main findings of the present work can be summarized as follows: (a) rhodium-assisted in situ formation of new C-, N-, and S-coordinating ligand (L^{2-}) via C−H and C−S bond scissions; PPh_3 plays a crucial role in the latter bond-breaking process. (b) The preferred pathway for S−C(sp^3) bond cleavage of the coordinated thioether moiety is likely to be the reductive cleavage by SET mechanism. (c) The superior nucleophilicity of thiolato group can be exploited to assemble electronically as well as coordinatively saturated compounds; **5** appears as a viable precursor to tailored S-bridged dimers **7** and **8**. (d) Phosphine mediated monomer−dimer interconversion of hexacoordinated rhodium thiolates. (e) Unlike thioether and μ-S bridged dinuclear species, mononuclear thiolato complex exhibits a fully reversible oxidative response that is supposed to be primarily centered on the thiophenolate sulfur atom. EPR spectroscopy of the oxidized form formed by electrochemical means along with DFT study reveal the formation of rhodium-bound thiyl radical cation $\mathbf{5}^{\bullet+}$. (f) Noncovalent "phenyl−phenyl" and "metallochelate−metallochelate" interactions are important toward the stabilization of sterically unfavorable syn isomer **8**.

(37) (a) Mueting, A. M.; Boyle, P.; Pignolet, L. H. *Inorg. Chem.* **1984**, *23*, 44−48. (b) Bianchini, C.; Mealli, C.; Meli, A.; Sabat, M. *Inorg. Chem.* **1986**, *25*, 4617−4618. (c) Dilworth, J. R.; Morales, D.; Zheng, Y. *J. Chem. Soc., Dalton Trans.* **2000**, 3007−3015. (d) Seino, H.; Yoshikaya, T.; Hidai, M.; Mizobe, Y. *J. Chem. Soc., Dalton Trans.* **2004**, 3593−3600.

(38) Janiak, C. *J. Chem. Soc., Dalton Trans.* **2000**, 3885−3896.

We anticipate that this information will guide the preparation of the analogous systems for other noble metals. Work is now in progress to prepare a new class of organothiolates and discover their reactivity.

Acknowledgment. We thank the Department of Science and Technology, New Delhi, for financial assistance (Grant SR/FTP/CS-20/2005), and data collection of two crystals on CCD facility setup (IISc, Bangalore, India) under the IRPHA-DST program. This research has also been funded by Jadavpur University. We thank Mr. Vivek Dhyani, PerkinElmer India, for the GC/MS experiment. We thank Dr. K. K. Rajak, Jadavpur University, for help in computations. B.A. thanks the UGC, New Delhi, for his fellowship.

Supporting Information Available: Crystallographic data (CIF) for **5**, **6b**, **7**, and **8**, structural data for **1** ($R = CH_2Ph$), characterization data, and structural analysis of **8**. This material is available free of charge via the Internet at http://pubs.acs.org.

IC7016006